CHAPTER 1

Introduction to the Application of Nitrides, Carbides, Phosphides and Amorphous Boron Alloys in Catalysis

KEVIN J. SMITH

Department of Chemical and Biological Engineering, University of British Columbia, 2360 East Mall, Vancouver, BC V6T 1Z3, Canada
Email: kjs@mail.ubc.ca

1.1 Introduction

Catalysts are used to enhance the rates of thermocatalytic, electrocatalytic and photocatalytic reactions.[1] Catalysts function by interacting with reacting species to generate new reaction intermediates that only exist on the catalyst surface, thereby providing alternative, faster reaction pathways to the desired products. Key to the catalytic reaction is the breaking and forming of new bonds between the catalyst and the reacting molecules. Consequently, the efficacy of a particular catalyst is determined by its surface chemistry and new developments in catalysis science and technology are driven in part by the development of new materials with well controlled surface properties. Increasing attention has been given to the discovery of heterogeneous catalysts that have high thermal and chemical stability, using materials that are not strategically limited and are of low cost.[2] Catalysts are used in a wide range of applications including motor vehicle emissions control, upgrading and

Catalysis Series No. 34
Alternative Catalytic Materials: Carbides, Nitrides, Phosphides and Amorphous Boron Alloys
Edited by Justin S. J. Hargreaves, Andrew R. McFarlane and Said Laassiri

Published by the Royal Society of Chemistry, www.rsc.org

refining of crude oils, and they are responsible for approximately 90% of the chemical processes currently operating world-wide in the chemical industry.[1,3]

Controlling the reactivity of a catalyst surface plays a key role in obtaining catalysts with high activity and selectivity. Sabatier's principle indicates that the interactions between reacting species and a catalyst surface must be of the appropriate strength—interactions that are too strong or too weak yield less active catalysts.[1] Hence, in the classic paper of Levy and Boudart,[4] C added to W to produce W_2C, was shown to decrease the high reactivity of W toward O and thereby yield an effective catalyst for the $H_2 + O_2 \rightarrow H_2O$ reaction at room temperature, a reaction typically catalysed by Pt. Similarly, the W_2C was active for the isomerisation of 2,2-dimethylpropane to 2-methylbutane, a reaction also catalysed by Pt.[4] This work spawned a large number of studies in which new materials with metallic character, formed by the incorporation of C, N, P and B into the lattices of early transition metals, have been investigated as potential catalysts for various reactions.[5–7] These interstitial alloys adopt simple crystal structures with the carbides and nitrides forming face-centered cubic (fcc), hexagonal close packed (hcp) or simple hexagonal (hex) structures, as summarised in Table 1.1. Many metal phosphides are also known[7] and their crystal structures as shown in Figure 1.1. The very rich chemistry of these interstitial alloys provides an opportunity for the development of new catalysts with a wide potential for application, especially with the synthesis of these materials as well dispersed nanoparticles.[5]

The unique catalytic behaviour of metals bound to C, N, P or S may be attributed to the changes in the electronic properties of the metal surface induced by the ligands and/or the geometry by which the metal and the ligands are arranged at the catalyst surface. Hence, the ligands passivate the metal surface reactivity and these effects have been quantified in some cases using molecular simulation.[10] For example, Liu and Rodriguez[11] have shown, by DFT calculation, that the CO adsorption and S adsorption energies on the (001) surfaces of MoN, MoC, MoP and Mo decrease with an increase in their d-band centre energy, as shown in Figure 1.2.

These observations suggest the possibility that metal surface reactivity can be controlled and tuned using interstitial atoms.[12] Consequently, there exist several detailed reviews describing the incorporation of C,[5,13] N,[6,14] P[7,9] and B[15] into metals and the use of the resulting interstitial alloys for catalysis, with varying degrees of success. Since, in nearly all cases, the interstitial atoms are incorporated into metals, the application of these new materials is

Table 1.1 Common Crystal Structures of Selected Carbides and Nitrides. Adapted from ref. 5 and 8.

Crystal structure	Compound
Fcc	TiC, ZrC, HfC, VC, NbC, and TaC TiN, VN, NbN γ-Mo_2N, β-W_2N, Re_2N
Hcp	β-Mo_2N, W_2C, Re_2C
Hexagonal	WC, MoC, δ-WN

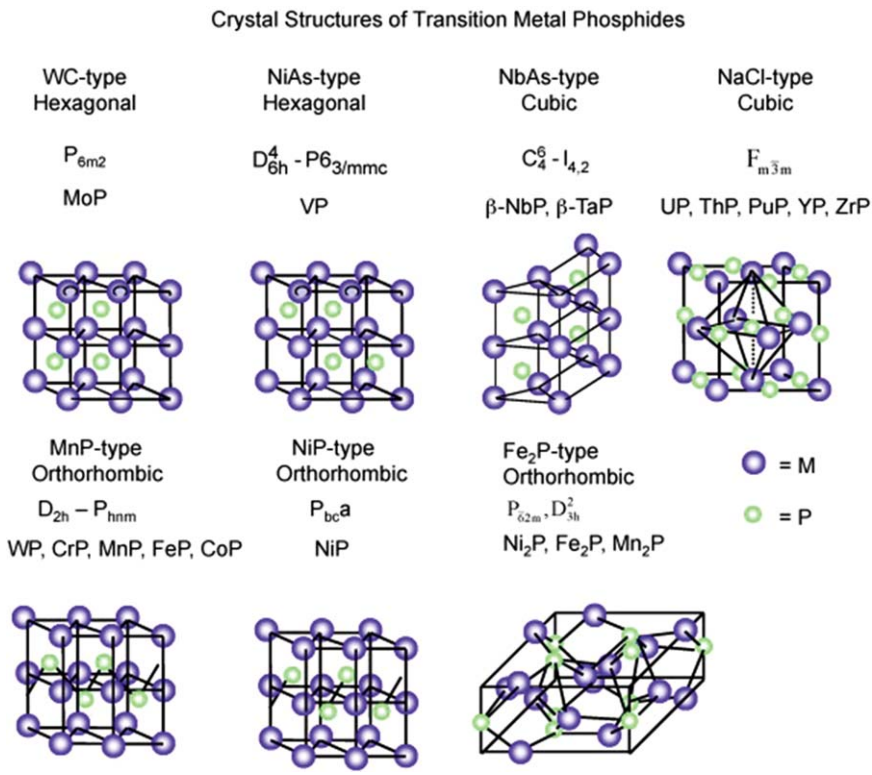

Figure 1.1 Crystal structures of metal-rich phosphides.[9]
Reprinted from *Catal. Today,* **143**, S. T. Oyama, T. Gott, H. Zhao and Y. Lee, Transition metal phosphide hydroprocessing catalysts: A review, 94–107. Copyright (2009) with permission from Elsevier.

mostly focused on reactions catalysed by metals. In some cases, however, the catalysts may also have acidic or basic properties, broadening their potential application.[16–18] In this chapter, the application of these materials is introduced with a view to demonstrating the wide scope of their application in heterogeneous catalysis. The focus is on their use as thermochemical catalysts and electrocatalysts, although they have also been used as catalyst supports. Selected examples are described to illustrate the application. Comprehensive reviews of these materials and their applications are presented in later chapters.

1.2 Hydrogenation Reactions

Hydrogenation reactions that use expensive metal catalysts are an essential part of chemical synthesis and product upgrading processes.[3] Metal carbides,[19–22] nitrides[23–25] and especially borides[26–28] are also effective hydrogenation catalysts for a wide range of applications and these materials have the potential to replace some metal catalysts.

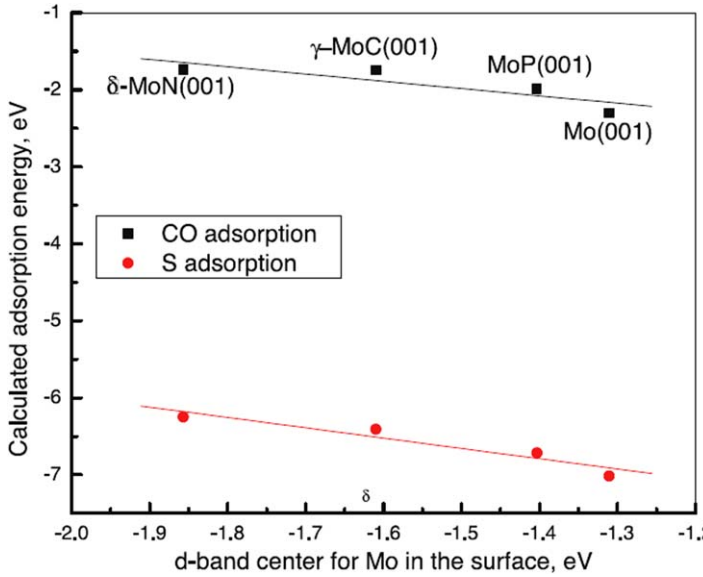

Figure 1.2 Calculated adsorption energy of CO (g) and S (*l*) as a function of the d-band centre for Mo in clean surfaces of Mo(001), γ-MoC(001), δ-MoN(001) and MoP(001). Here, the d-band centres are relative to the Fermi energy.[11]
P. Liu and J. A. Rodriguez, *Catalysis Letters*, 2003, **91**, 247–252. With permission of Springer.

The hydrogenation of aromatic compounds is possible on metal carbide, nitride, phosphide and boride catalysts. Mo_2C has been shown to hydrogenate naphthalene to tetralin with high selectivity (>90%) at 340 °C and 4 MPa H_2, although catalyst activity declined from 90% to 30% over a period of about 60 h.[29] When supported on HY zeolite, the Mo_2C also shows some ring-opening activity with about 10% selectivity to ring-opened products and 80% tetralin selectivity at 300 °C and 3 MPa H_2.[30] However, the Mo_2C/HY catalyst was less active than a commercial Pd/HY catalyst operated at the same conditions. The bimetallic nitride Ni_2Mo_3N (unsupported) also has high catalytic activity for benzene hydrogenation[25] and promotion with K reduces the deactivation of the catalyst in the presence of S.[31] Amorphous RuB supported on ZrO_2 hydrogenates benzene to cyclohexene with high yields (46% maximum at 433 K, 5 MPa and 55 min reaction time and liquid phase).[32]

The hydrogenation of toluene on a low surface area (12 $m^2 g^{-1}$) unsupported Mo_2C has also been reported at 423–598 K and 2.76 MPa H_2 pressure. Within the temperature range 473–523 K, the yield of methylcyclohexane was 100%, but at higher temperature, ethylcylopentane was also produced as a result of isomerisation reactions.[33] The dehydrogenation of decalin has also been shown to occur on WC,[34] while the dehydrogenation performance of a Ni–WC/AC catalyst was better than that of Ni/AC and WC/AC at 101 kPa and 400 °C. Among a series Ni–WC/AC catalysts, decalin

dehydrogenation to naphthalene was highest on a 30 wt%Ni–20 wt%WC/AC catalyst. The Ni–WC/AC catalyst showed good stability for decalin dehydrogenation.[34] The hydrogenation of olefins and dienes has also been reported on amorphous metal borides,[35–37] nitrides[23,38] and carbides.[23]

In the past decade, the transformation of residual biomass into fuels and chemicals has been the focus of much research. Hydrogenations of intermediate molecules is an important step in these processes and the Pt-group metals (PGMs) are often the catalyst of choice for the hydrogenation reactions. For example, levulinic acid (LA) has been identified as an important molecule for application in future biorefineries that can be produced from lignocellulosic wastes at low cost. LA can be hydrogenated to γ-valerolactone (GVL), which also has many potential applications. The heterogeneous catalytic hydrogenation of LA to GVL is therefore of interest and Ru supported on activated carbon is usually the catalyst of choice. Recently, Quiroz *et al.*[39] reported that nanostructured β-Mo_2C has a LA to GVL turnover frequency (TOF) of 2.3 min^{-1}, measured at 30 bar H_2 and 180 °C, the same order of magnitude as that reported for Ru/TiO_2 (9.8 min^{-1})[40] and a Ni–MoO_x/C (TOF of 3.4 min^{-1}), the latter performed under more severe conditions (50 bar H_2 and 240 °C).[41] The authors also reported that the nanostructured β-Mo_2C was stable under continuous operation. Amorphous metal-boride alloy catalysts have also attracted attention for hydrogenation of bio-based feedstocks. The hydrogenation of furfural, crotonaldehyde and citral on CuB/SiO_2 and $Cr–CuB/SiO_2$ catalysts, has been carried out with 5 mL of substrate in 75 mL ethanol at 393 K for furfural and crotonaldehyde, and at 373 K for citral, under a constant pressure of 929 kPa.[42] The CuB/SiO_2 catalyst was more active than a Cu/SiO_2 catalyst. Citral hydrogenation on a 5%NiB/SiO_2 catalyst has a high yield (~84%) at 30 °C.[43] In the hydrogenation of fructose and fructose/glucose mixtures, bimetallic amorphous CoNiB catalysts operated at 343 K and 6 MPa were more active than NiB, and much more active than CoB and Raney Ni.[44] In a separate study of glucose hydrogenation over an amorphous $Ni–B/SiO_2$ catalyst at 373 K and 4.0 MPa, the catalyst had much higher activity than other Ni-based catalysts, including crystalline $Ni–B/SiO_2$, Ni/SiO_2 and a commercial Raney Ni catalyst.[45,46] The hydrogenation of ethyl lactate derived from fermentation of renewable resources such as carbohydrates, to yield a green propanediol can also be achieved on a RuB/Sn-SBA-15 catalyst operated at 423 K and 5.5 MPa H_2.[47]

The carbides, nitrides and borides have also been shown to have high activity and selectivity for the hydrogenation and reduction of nitro groups.[20,48,49] The bimetallic nitride Fe_3Mo_3N promotes selective reduction of $–NO_2$ in *p*-chloronitrobenzene to generate *p*-chloroaniline whereas Co_3Mo_3N favours C–Cl scission with the formation of nitrobenzene.[25] Earlier work has also shown that the transition metal nitrides have activity for *n*-butane dehydrogenation, hydrogenolysis and isomerisation.[50] Hydrogenation of *p*-chloronitrobenzene also occurs on La-doped NiMoB,[51] NiFeB[52] and NiCoB.[53]

Metal carbide catalysts have also been shown to be effective in the hydrogenation of dimethyl oxalate (DMO) to ethanol.[54,55] This indirect synthesis route to ethanol, uses CO oxidative coupling to produce DMO. The authors report that Cu–Mo_2C/SiO_2 and Mo_2C/SiO_2 have very good stability and activity for the hydrogenation of DMO to ethanol (Figure 1.3) at low temperatures (473 K), compared to conventional Cu/SiO_2, which although very active, degrades during hydrogenation because of agglomeration of the Cu particles.

1.3 Hydrotreating Reactions

Hydrotreating refers to a class of reactions in which heteroatoms (S, N, O) are removed from organic molecules by reaction with hydrogen to yield refined products suitable for use as fuels and chemicals.[56] Conventional hydrotreating catalysts are based on supported MoS_2 promoted with Co or Ni. These catalysts have been used commercially in the petroleum industry for decades, especially for hydrodesulfurisation (HDS) and hydrodenitrogenation (HDN) processes.[3,56] With increased environmental legislation that has reduced allowable S and N levels in fuels, catalysts with higher HDN and HDS activity, especially for the more refractory heteroaromatics present in residue oils, has become the focus of research and in this regard, metal carbides,[13] nitrides,[13,14] and phosphides[9,57] have been applied to both HDS and HDN. In the HDS of thiophene at 450 °C, both Co_2B and Ni_3B are partially sulfided,[58] suggesting that the borides are unstable and for this reason there are few studies describing the catalytic activity of metal borides for HDN and HDS. With the growing interest in bio-oil upgrading in which O removal by hydrodeoxygenation (HDO) reactions is critical, the carbides, nitrides, phosphides and borides have also been assessed for HDO.[6,59,60]

Table 1.2 reports data from Sajkowski and Oyama[61] who compared the hydrotreating activity of a commercial Ni–MoS/Al_2O_3 catalyst to that of a Mo_2N and a Mo_2C/Al_2O_3 catalyst. The catalysts were assessed using a residue oil and a gas oil, both derived from coal, so that the feedstocks had high S (810 and 116 ppm S, respectively) and N (4620 and 3580 ppm N, respectively) contents. The apparent first-order rate constants for desulfurisation, denitrogenation and aromatic saturation reactions, normalised for the number of active sites measured by suitable chemisorption experiments, show the Mo_2C to be significantly more active than the commercial catalyst.

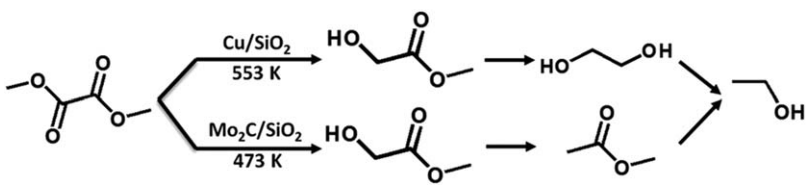

Figure 1.3 The reaction pathway of the hydrogenation of DMO. Reproduced from ref. 54 with permission from The Royal Society of Chemistry.

Table 1.2 Estimated relative first-order rate constants per active site, adapted from Sajkowski and Oyama.[61] Results measured at 633 K and 13.7 MPa with co-current upward flow of oil (4 $cm^3\,h^{-1}$) and H_2 (159 cm^3 (STP) min^{-1}).

	Desulfurisation	Denitrogenation	Aromatic saturation
Mo_2N	1.3	3.4	3.4
Mo_2C/Al_2O_3	2.1	5	3.1
MoS_2/Al_2O_3	0.67	0.98	0.41
$Ni–Mo–S/Al_2O_3$	1	1	1

However, in a comparison of NiMo sulfide, carbide and nitride catalysts for the HDS of thiophene and Maya crude oil, Villasana *et al.*[62] reported that NiMoS was the most effective catalyst and this trend was the same for residue conversion.[62] The HDN and HDS activities of bimetallic Ni–Mo carbide, nitride and sulfide catalysts have also been compared using light gas oil and heavy gas oil derived from Athabasca bitumen at 8.8 MPa in the temperature range 340–370 °C and 375–400 °C, respectively. The supported Ni–Mo sulfide catalyst was more active for HDN and HDS of light gas oil and heavy gas oil than the corresponding carbide and nitride catalysts, on a mass of catalyst basis.[63–65] In another study, P-promoted Mo_2C/Al_2O_3 was shown to be more active for deep desulfurisation of refractory compounds such as 4,6-dimethyldibenzothiophene than a commercial Ni–Mo sulfide.[66] The metal phosphides are also effective for hydrotreating real feedstocks, as demonstrated by Oyama *et al.*[57,67] who reported that Ni_2P/SiO_2 had better activity in hydroprocessing than a commercial $Ni–Mo–S/Al_2O_3$ catalyst when using a real gas oil feed at 593 K and 3.9 MPa and based on equal catalyst weights loaded in the reactor (HDS 85% *vs.* 80%). Subsequent studies also reported significant activity of bimetallic phosphides using realistic gas oil feedstocks.[68–70] The gradual transformation of Ni–Mo carbide, nitride and phosphide phases into Ni–Mo sulfide phases was observed during the hydrotreating reactions and similar transformations have been reported in other studies.[31,58,62] The impact of changes in composition and morphology on the long-term operation of these alternative catalysts under commercial conditions has not been reported in the literature, but these transformations likely impact the reported relative activity of the materials among the different studies.

Many other studies have demonstrated that the metal carbides, nitrides and phosphides are effective catalysts for HDS and HDN reactions using model reactants. Studies with model compounds allow reaction pathways to be clearly established. For example, in studies of the deep desulfurisation of refractory heteroaromatics on Mo_2C,[66,71] in which 4,6-dimethyldibenzothiophene (4,6 DMDBT) is used as model reactant, it was shown that the reaction proceeds by two parallel routes leading to 3,3′-dimethylbiphenyl (DMBP) by a direct desulfurisation (DDS) pathway or to 3-(3′-methylcyclohexyl)toluene (MCHT) through a hydrogenation (HYD) pathway, as summarised in Figure 1.4.[72] On the Mo_2C catalyst, the DDS route is more important (HYD/DDS = 0.7) whereas over commercial $Ni–Mo–S/Al_2O_3$,

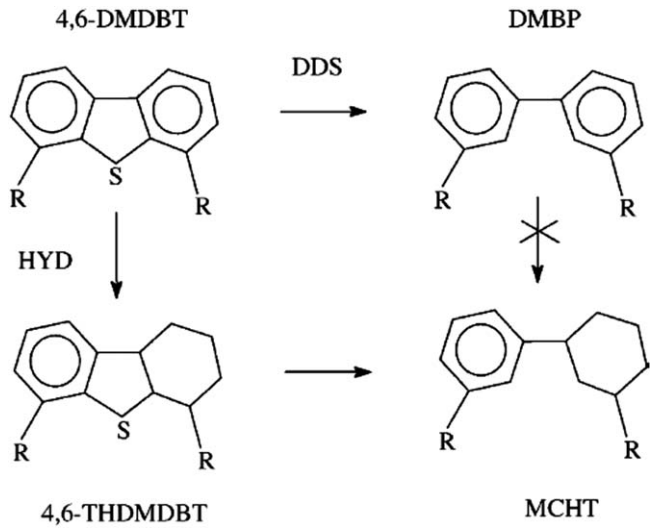

Figure 1.4 Pathways for HDS of 4,6DMDBT.[72]
Reprinted from *J. Mol. Catal. A: Chem.*, **184**, P. Da Costa, C. Potvin, J.-M. Manoli, J.-L. Lemberton, G. Perot and J. Djega-Mariadassou, New catalysts for deep hydrotreatment of diesel fuel: Kinetics of 4,6-dimethyldibenzothiophene hydrodesulfurisation over alumina-supported molybdenum carbide, 323–333. Copyright (2002) with permission from Elsevier.

operating under the same conditions of temperature (613 K) and pressure (4 MPa total pressure), the HDS of 4,6-DMDBT by the HYD pathway is favoured (80% for Ni–Mo–S/Al_2O_3).[72] In another important study, a series of transition metal carbides (Mo_2C, WC, NbC) and nitrides (TiN, VN, Mo_2N) were tested in a three-phase trickle-bed reactor using a model liquid feed mixture containing 3000 ppm sulfur (dibenzothiophene), 2000 ppm nitrogen (quinoline), 500 ppm oxygen (benzofuran), 20 wt% aromatics (tetralin), and balance aliphatics (tetradecane).[73] The Mo_2C showed higher HDN activity than a commercial sulfided Ni–Mo/Al_2O_3 catalyst (on the basis of unit area of catalyst), while VN was found to exhibit excellent activity and selectivity for the HDO of benzofuran. The HDN activity of WC was found to be comparable to that of a commercial sulfided Ni–Mo/Al_2O_3 catalyst. A comparative study of the metal phosphides using dibenzothiophene as the model reactant for HDS and quinoline for HDN at 643 K and 3.1 MPa, showed the order of activity increased as follows: $Fe_2P < CoP < MoP < WP < Ni_2P$,[57] on the basis of an equal number of active sites in the reactor. Few studies of HDN using metal nitrides other than Mo_2N have been reported in the literature.[14] Milad *et al.*[74] reported that the activity per unit area of a series of unsupported metal nitrides for pyridine HDN was as follows: $Co_4N > Fe_3N > Mo_2N > W_2N > NbN > CrN > VN$. The activity of the metal nitrides decreased with the heat of formation of the metal nitrides.

Despite the promising activities of the metal carbides, nitrides and phosphides reported in the literature for the HDS and HDN reactions, these

are well established, mature commercial technologies used to produce high quality fuels and it is difficult to displace the highly active Ni(Co)–Mo–S/Al_2O_3 catalysts that have been optimised for these processes over many years. However, with increased interest in the development of biorefinery technology for sustainable green fuels, and given that one major route to green fuels involves O-removal from intermediate bio-oils generated by pyrolysis processes,[75] there has been a very significant effort to demonstrate the use of metal carbide,[76–78] nitride[79–81] and phosphide[82,83] catalysts for HDO reactions.[84] There are several examples in the literature where the carbides, nitrides and phosphides are shown to favour reaction pathways for O removal that are different to that which occurs on group 8 metal catalysts.[76,85] For example, with phenol as a model reactant on metals such as Pt, Pd and Rh, hydrogenation reactions dominate, yielding cyclohexanol as product; whereas, on metals with higher O affinities such as Ru, Co and Ni, deoxygenation reactions occur more readily.[86] On Mo_2C and W_2C, C–O bond cleavage is favoured with minimal hydrogenation occurring especially on oxygen-modified materials.[76] Studies of the HDO of guaiacol (Figure 1.5) show that a key first step in the HDO over Ru, for example, is *via* catechol formation (by O–CH_3 bond cleavage) followed by phenol formation (R–OH bond cleavage),[85,87] whereas on Mo_2C direct demethoxylation occurs to yield phenol.[76] The same demethoxylation reactions occur on transition metal phosphide catalysts[82] whereas both paths appear to occur on Mo_2N.[79]

Although the unique characteristics of these materials for the HDO of model compounds is well documented, few studies of their application

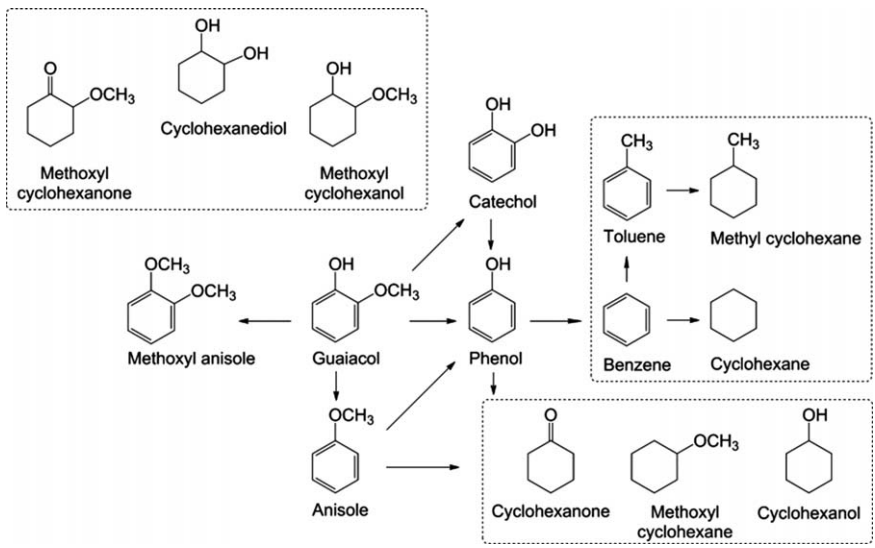

Figure 1.5 Reaction network for guaiacol conversion as reported by Chang *et al.*[85] Reprinted with permission from ref. 85. © 2013 WILEY-VCH Verlag GmbH & Co. KGaA, Weinheim.

using real bio-oils are available. Recently, however, Guo *et al.*[88] compared a series of metal phosphides for the HDO of a pyrolysis oil at 300 °C and 50 bar, using 40 g of pyrolysis oil and 2 g of catalyst reacted for 3 h (Figure 1.6). The authors reported that MoP/AC had HDO activity comparable to a Ru/C catalyst and the HDO activity of the metal phosphides were found to follow the order of NiP/AC > CoP/AC > MoP/AC.[88] Figure 1.6 also shows that the oil fraction yield was significantly improved by addition of P and the MoP/AC catalyst had the highest oil fraction yield among the Mo-based catalysts.

Hydrotreating vegetable oils mainly composed of triglycerides is another important deoxygenation pathway to prepare high-grade diesel-like hydrocarbons from renewable biomass.[89] Several studies have investigated metal carbides,[90,91] nitrides[92] and phosphides[93,94] for the HDO of vegetable oils. Table 1.3 compares results from various vegetable oils using a Mo_2C catalyst and Table 1.4 gives a comparison among Mo_2N, WN and VN supported on γ-Al_2O_3 used in the hydrotreating of oleic acid.[92] The Mo_2C catalyst shows high yields of deoxygenated hydrocarbons for a range of vegetable oils, whereas Table 1.4 shows similar activity for the Mo_2N catalyst, with the VN having significantly lower yield of hydrocarbon products. HDO of methyl palmitate (50% in decalin) over a 5–20 wt% Ni_2P/MCM catalyst at 3 MPa H_2, WHSV = 3 h^{-1}, and H_2/oil = 1000 at 290–350 °C has also been reported.[93] At 290 °C, the conversion was 85% with C_{15} and C_{16} selectivities of 55% and 45%, respectively. The HDO of methyl laurate at 573–613 K and 3.0 MPa on Ni_2P on various supports was reported by Shi *et al.*,[95] showing that the

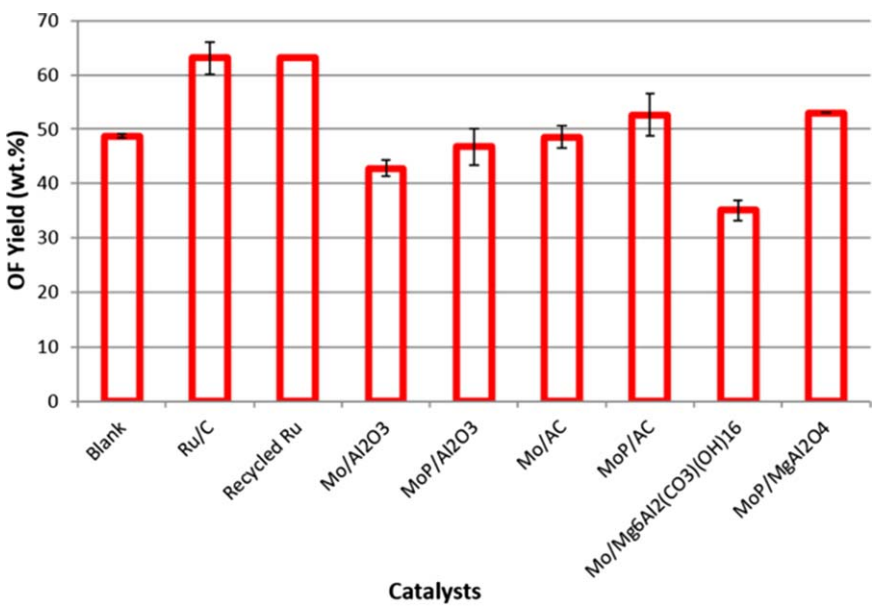

Figure 1.6 Yield of oil fraction from the HDO experiments with different in-house prepared catalysts compared with the commercial Ru/C catalyst (300 °C, 50 bar H_2, 3 h).[88] © 2016 American Institute of Chemical Engineers.

Table 1.3 Catalytic performance of 5% Mo_2C supported on ordered mesoporous carbon (OMC) and reacted at 260 °C in 2.0 MPa H_2 for 3 h. Adapted from ref. 91.[a]

Vegetable oil	Conversion (%)	Yield (%)
Maize oil	100	95
Olive oil	100	95
Rapeseed oil	88	85
Soya bean oil	94	92
Sunflower oil	97	94

[a]Note: The yield was defined as the mass of hydrocarbons produced (mainly in the range of C_{15}–C_{18}) divided by the mass theoretically produced.

Table 1.4 Metal nitride catalysts supported on γ-Al_2O_3 for hydrotreating oleic acid at 380 °C, 7.15 MPa H_2, 0.45 h^{-1} and 810 H_2/L oleic acid. Adapted from ref. 92.

	Mo_2N	WN	VN
Oleic acid conversion (%)	99.9	97.1	97.0
O removal (%)	~100	~100	71.8
Product yields (g/100 g oleic acid)			
Liquid organic products	84.1	81.1	85.0
CO_2	1.6	2.2	2.6
H_2O	9.7	4.2	2.4

conversion of methyl laurate and the selectivity to C_{11} and C_{12} hydrocarbons was highest on the Ni_2P/SiO_2 catalyst. The effect of the support mainly results from the support acidity and the metal-support interaction that limits reducibility.[95] The high activity of the Ni_2P for O-removal compared to other metal phosphides has also been observed for HDS and HDN reactions.

In a related study, the bulk metal-rich phosphide, Ni_3P, prepared with high purity using a hydrothermal method followed by annealing at 773 K,[96] has been shown to have high activity for selective glycerol hydrogenolysis at low temperature, with high selectivity to 1,2-propanediol.[96]

The direct catalytic conversion of raw woody biomass into phenols and diols over a carbon supported Ni-W_2C catalyst has also been reported (Table 1.5).[97] Using various sources of woody biomass, catalyst and 100 mL of water reacted at 235 °C and 6 MPa H_2 for 4 h, the carbohydrate fraction in the woody biomass was converted to ethylene glycol and other diols. A synergistic effect in Ni–W_2C/AC existed, not only in the conversion of the carbohydrate fraction, but also in lignin component degradation and the latter activity was comparable to noble metal catalysts.

In another potential application, the catalytic conversion of Kraft lignin by ethanolysis was reported over a α-MoC_{1-x} catalyst supported on activated carbon (AC).[98] The reaction was done in supercritical ethanol at 280 °C for 6 h in the absence of H_2. Products included C_6 monohydric alcohols, C_8–C_{10} esters, C_7–C_{10} monohydric phenols, C_7–C_{10} benzylalcohols, and C_8–C_{10} aromatic hydrocarbons. No oligomers or char were formed and both the

Table 1.5 The results of 4% Ni-30% W_2C/AC catalysed hydrocracking of different sources of woody biomass at 235 °C and 6 MPa H_2. Adapted from ref. 97.

Biomass source	Phenol yield (%)	Diol yield (%)
Poplar	32	75
Baswood	37	71
Ashtree	41	76
Beech	26	58
Xylosma	29	62
Bagasse	23	60
Pine	10	44
Yate	11	31

Table 1.6 Product yields from lignin conversion using WP catalysts at 553 K and 2 MPa H_2. Adapted from ref. 99.

Catalyst	Phenol selectivity	Product yield ($mg\,g^{-1}$)	
		Sulfur ethers	Phenols
None	72.6	7.4	19.6
WP	66.6	22.4	44.6
WP/SiO_2	54.1	26.0	30.7
WP/AC	51.7	62.5	67.0
Ni-WP/AC	73.1	18.0	48.8
Fe-WP/AC	75.3	17.3	52.7

solvent and catalyst affect the molecular yields and product composition. Wheat-straw Kraft lignin from black liquor can also be used as the feed.

In related work, the direct catalytic decomposition of alkaline lignin over WP catalysts in a hot compressed water–ethanol mixed solvent has also been reported (Table 1.6).[99] The reactor was loaded with alkaline lignin (1.0 g), fresh catalyst (0.3 g) and a mixture of water and ethanol solvent (volume ratio 1 : 1, total 100 mL), pressurised to 2.0 MPa H_2 and reacted at 553 K for 2 h. The products from the WP/Carbon catalyst consisted of 2-methoxy-phenol (guaiacol), 2-methoxy-4-methyl-phenol, 2-methoxy-4-ethyl-phenol, 2-methoxy-4-acetyl-phenol and 2-methoxy-4-propyl-phenol. The highest overall phenol yield was 67.0 $mg\,g^{-1}$ lignin.[99]

Carbide catalysts have also been used for the conversion of cellulose to polyols, especially to ethylene glycol (EG). The catalytic performance of tungsten carbides, molybdenum carbides and platinum on carbon supports reacted at 518 K and 6 MPa for 30 min is summarised in Table 1.7.[100] Among all the catalysts, tungsten carbide supported on activated carbon, W_2C/AC, showed a higher yield of EG than the Pt, Ni or Mo_2C catalysts and the highest EG yield (61%) occurred with the Ni-promoted W_2C.

1.4 Synthesis Gas Production

The metal carbides, nitrides and phosphides have been shown to be effective for a range of reactions involving molecules with one carbon atom, such as

Table 1.7 Cellulose conversion and polyol yields over different catalysts at 518 K and 6 MPa for 30 min. Adapted from ref. 100.

Catalyst	Conversion (%)	EG yield (%)
Pt/AC	66	8.2
Ni/AC	68	5.2
W_2C/AC	98	27.4
Mo_2C/AC	85	5.3
2%Ni-W_2C/AC	100	61.0
2%Ni-Mo_2C/AC	87	11.3

Table 1.8 Dry reforming of methane over supported Mo_2C catalysts operated at 1220 K, 8 bar $CH_4/CO_2 = 1$ and GHSV = 2600 h^{-1}. Adapted from ref. 102.

Catalyst support	Mo_2C loading (wt%)	Conversion (%)		CO Yield (%)	H_2/CO
		CH_4	CO_2		
SiO_2	18.3	91	86	89	0.95
γ-Al_2O_3	12.5	89	86	87	0.97
ZrO_2	6.5	90	93	92	0.96
TiO_2	10.1	31	27	29	—

CO_2, CO and CH_4, although most applications have focused on the metal carbides. The production of synthesis gas from CH_4 is possible by steam reforming, dry reforming, or partial oxidation yielding a synthesis gas with a H_2/CO ratio close to 3, 1 or 2, respectively. Depending on the application, additional processing steps are required to adjust the H_2/CO ratio to the desired value. Given the search for new technologies for the conversion and capture of CO_2, there is a growing interest in the dry reforming of CH_4 and Mo_2C catalysts are active for this reaction.[101] High activity of Mo_2C on various oxide supports was reported by Brungs *et al.*,[102] as summarised in Table 1.8. The relative stability of the catalysts is reported as $Mo_2C/Al_2O_3 > Mo_2C/ZrO_2 > Mo_2C/SiO_2 > Mo_2C/TiO_2$. Subsequent studies have investigated several other metal carbides as catalysts for dry reforming, as is summarised in Table 1.9.

Combined reforming technologies including bi- and tri-reforming of CH_4 have also attracted interest owing to the elimination of the need for a secondary process to adjust the H_2/CO ratio to the required value.[103–106] Small amounts of Mo_2C (0.5–2 wt%) added to Ni/ZrO_2 catalysts were reported to be beneficial for increasing the catalyst activity of the steam-CO_2 bi-reforming of CH_4 and the increased activity was ascribed to an increased Ni dispersion and a higher Mo(II) content of the catalyst.[106] The best catalyst, with 0.5 wt% Mo_2C–10 wt% Ni/ZrO_2 also had higher stability in comparison with an unmodified 10 wt% Ni/ZrO_2 catalyst.[106] The ability of Ni/Mo_2C to catalyse CH_4 bi-reforming at 950 °C has also been demonstrated.[107] A rapid loss in activity of the catalyst was noted after a certain reaction period, after which Mo_2C oxidation to MoO_2 occurred, but no evidence of coking, the usual limitation

Table 1.9 Summary of carbide catalysts for dry reforming of CH_4.

Catalyst	Temperature (°C)	Pressure (kPa)	CH_4/CO_2 feed ratio	CO_2 conv. (%)	CO yield (%)	Ref.
5%Ni/βSiC	900	101	1	90	—	164
5%Mo_2C/ZrO_2	950	101	1	58	—	165
5%Mo_2C–1%Bi/ZrO_2	950	101	1	75	—	165
Co_6W_6C	850	404	1	70	42	166
Ni–Mo_2C/La_2O_3	800	110	1	78	—	167
20Co–Mo_2C/ZrO_2	850	101	1	97	87	168
Ni–WC	800	101	1	90	80	169
Ni–Mo_2C	800	101	1	90	80	169

in dry reforming reactions, was observed.[107] Tri-reforming in which the three reactions:

$$\text{Dry reforming:} \quad CO_2 + CH_4 \rightarrow 2CO + 2H_2 \ (\Delta H^\circ = 247.3 \text{ kJ mol}^{-1})$$
$$\text{Steam reforming:} \quad H_2O + CH_4 \rightarrow CO + 3H_2 \ (\Delta H^\circ = 206.3 \text{ kJ mol}^{-1})$$
$$\text{Partial oxidation:} \quad CH_4 + 1/2O_2 \rightarrow CO + 2H_2 \ (\Delta H^\circ = -35.6 \text{ kJ mol}^{-1})$$

occur simultaneously to yield synthesis gas, has also been described using Ni–Mg catalysts supported on SiC.[104,105]

Several studies have focused on Mo_2C for the water–gas shift (WGS) or the reverse water–gas shift (RWGS) reaction: $CO + H_2O \rightleftharpoons CO_2 + H_2O$. When steam reforming of CH_4 is used for the industrial production of hydrogen from CH_4 ($CH_4 + 2H_2O \rightarrow CO_2 + 4H_2$), the product stream usually contains small amounts (1–5%) of CO as an impurity and the WGS, catalysed by $Cu/ZnO/Al_2O_3$ catalysts, is used to remove the CO and produce additional hydrogen. Mo_2C has been shown to be a very effective support for Pt catalysts used to catalyse the WGS reaction.[108,109] The synthesised catalyst results in a unique interaction between the Pt and the Mo_2C raft like particles, and as shown in Figure 1.7, the rate of the WGS reaction for the Pt/Mo_2C is significantly higher than that for several other Pt catalysts supported on metal oxides.

In a subsequent study,[110] the metals Pt, Pd, Ni, Au, Ag and Cu supported on Mo_2C were also shown to have high activity for the WGS reaction. At 120 °C using a feed gas of 7% CO, 22% H_2O, 8.5% CO_2, 37% H_2, the WGS rate per unit area of catalyst for Pt, Au, Pd and Ni (1.5–2 wt%) supported on Mo_2C was 4–8 times higher than that of the commercial $Cu/ZnO/Al_2O_3$ catalyst.[110]

1.5 Synthesis Gas Conversion

Synthesis gas conversion to fuels and chemicals provides a route to clean fuels that are typically S-free. In addition, depending on the catalyst and chosen process, the products from synthesis gas can be varied from heavy

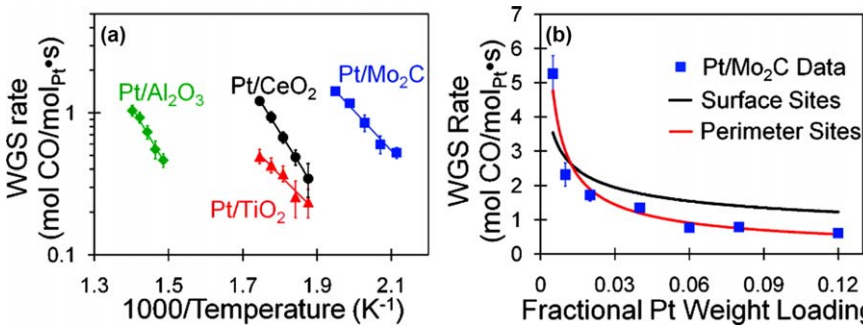

Figure 1.7 (a) Arrhenius plots of the WGS reaction rates for 2.7% Pt/Al_2O_3, 5% Pt/CeO_2, 2% Pt/TiO_2, and 4% Pt/Mo_2C catalysts. (b) WGS rates at 240 °C for the Pt/Mo_2C catalysts as a function of Pt loading including predicted rates from the surface site and perimeter site models.[108,109] Reprinted with permission from N. M. Schweitzer, J. A. Schaidle, O. K. Ezekoye, X. Pan, S. Linic and L. T. Thompson, *J. Am. Chem. Soc.*, 2011, **133**, 2378–2381. Copyright (2011) American Chemical Society.

waxes to CH_4 and may also include a range of oxygenated hydrocarbons, such as methanol and higher alcohols. The use of non-conventional metal carbides, nitrides, phosphides and the like have all been investigated for synthesis gas conversion.

The Fischer–Tropsch synthesis (FTS) converts synthesis gas into straight chain hydrocarbons by a surface polymerisation reaction with Fe[111] and Co[112] catalysts being used in industrial processes. Fe carbides, nitrides and carbo-nitrides were first studied in the 1950's,[113] with the nitrided iron catalysts showing significantly higher amounts of oxygenated hydrocarbons than the iron carbide. The catalysts also underwent significant structural and chemical changes upon exposure to the synthesis gas.[113] Other Fe-carbides synthesised by various methods are also known to be active for the FTS.[114,115] During FTS on Fe catalysts, the presence of Fe carbides is well known, with several different Fe-carbides being identified, including ε-Fe_2C, Fe_7C_3, χ-Fe_5C_2 and θ-Fe_3C.[116] Recently, the formation of θ-Fe_3C, χ-Fe_5C_2, and ε-Fe_2C was shown to depend on the thermodynamic stability of each phase at the gas phase composition and temperature of the reaction.[116] Furthermore, it was shown that a significant part of the Fe carbide phases were amorphous. The χ-Fe_5C_2 was oxidised during FTS conditions, and the θ-Fe_3C and amorphous carbide phases showed lower activity and selectivity than the other phases.

Other metal carbides, especially Mo_2C, are also known to have significant activity and selectivity for CO hydrogenation to methane[117,118] and other FTS products.[119–121] For example, CO hydrogenation at atmospheric pressure, 570 K with a 3/1 : H_2/CO ratio and SV of 10 000 h^{-1} on unsupported Mo_2C, produced mostly C_1–C_5 paraffins while promotion of the Mo_2C with K_2CO_3 yielded C_2–C_5 hydrocarbons with 80–100% olefins and reduced the methane selectivity.[119] Several promoters (K, Na, Co, Ce, Ba) have been

added to the Mo_2C catalyst in an attempt to control product selectivity with moderate success.[120–124] The use of Mo_2C catalysts for CO hydrogenation at high pressure to yield alcohols has also been extensively investigated.[10,125] According to Xiang *et al.*,[126] Mo_2C catalyst operated at $T = 573$ K, $P = 8.0$ MPa, GHSV = 2000 h^{-1}, $H_2/CO = 1.0$ yields mostly light hydrocarbons, whereas when the same catalyst is promoted with K_2CO_3, alcohols are also produced. At a K/Mo ratio of 0.2 the selectivity to alcohols (on a CO_2-free basis) was 53% whereas the hydrocarbon selectivity was 47%.[127] Adding Fe, Co or Ni to the K/Mo_2C catalysts resulted in an increase in catalyst activity in the order Ni > Co > Fe; whereas, in terms of C_{2+}OH selectivity (*i.e.* selectivity to alcohols above methanol) the increase was Ni > Co > Fe.[128] Ni-Mo bimetallic carbides operated at $H_2/CO = 2.0$, $T = 513$ K, $P = 7.0$ MPa, GHSV = 4000 h^{-1} also produce a product mix of alcohols and hydrocarbons that depends on the Ni content.[129] As summarised in Table 1.10, the addition of the Ni significantly increases selectivity to alcohols, with the hydrocarbon fraction dominated by more than 67% CH_4.[129] In one study, the effect of support was investigated for a K promoted Mo_2C catalyst, with CO conversion reaching a maximum with about 20 wt% Mo_2C loaded onto an active carbon support.[130] This study also demonstrated the need for the K promoter to be in contact with the Mo for effective promotion of the alcohols synthesis.[130]

Recent studies also report on metal nitrides, phosphides and borides as catalysts for synthesis gas conversion. Ultrafine catalysts of CuB and Me-CuB (Me = Cr, Th, Zr) have been investigated for methanol synthesis from CO/H_2[131] and CO_2/H_2.[132] In one example, 20% Zr–CuB (approximately 77% Cu by mass) operated at 250 °C, 3.0 MPa and CO_2/H_2 of 1 : 3 in the liquid phase with hexadecane as solvent, produced CH_3OH at a maximum selectivity of 55% and a CH_3OH synthesis rate of 1.5 mol kg_{Cu}^{-1} h^{-1}, equivalent to ~37 g CH_3OH kg_{cat}^{-1} h^{-1}.[132] At 150 °C, 6 MPa $H_2/CO = 2:1$ the CH_3OH synthesis rate was 46 mmol h^{-1} over the 20% Th-CuB catalyst (2 mmol Cu equivalent) in the presence of methylformate (80 mL) and potassium methoxide (3 g).[131] Synthesis gas conversion to mixed higher alcohols on metal phosphides was first investigated by Zaman and Smith,[133] in which synthesis gas conversion at 548 K, 8.3 MPa and a $H_2/CO = 1$ over a 10 wt% MoP/SiO_2 catalyst yielded mostly hydrocarbons with 35% selectivity to

Table 1.10 Performance of CO hydrogenation over the Ni–Mo bimetallic carbide catalysts operated at $H_2/CO = 2.0$, $T = 513$ K, $P = 7.0$ MPa, GHSV = 4000 h^{-1}. Adapted from ref. 129.

		Selectivity	
Catalyst	CO conv. (%)	ROH	CH_x
MoC	1.0	14.5	85.5
$Ni_{0.17}MoC$	35.0	46.5	54.0
$Ni_{0.5}MoC$	40.3	46.0	54.0
$Ni_{1.0}MoC$	41.1	34.6	65.4
$Ni_{2.0}MoC$	59.3	25.3	74.7

methane.[134] K addition to the MoP–SiO_2 shifted selectivity to oxygenates, with the highest oxygenate space time yield of 147.2 $g\,kg_{cat}^{-1}\,h^{-1}$ obtained over a 5 wt% K–15 wt% MoP–SiO_2 catalyst.[133,134] The highest selectivity towards C_2+ oxygenates (76.6 C atom%) and lowest selectivity towards CH_4 (9.7 C atom%) occurred on a 5 wt% K–10 wt% MoP–SiO_2 catalyst. The major oxygenates in the product were acetaldehyde, acetone and ethanol. Promotion of MoP by addition of Co and K has also been shown to improve selectivity to C_2+ oxygenates.[135] At 548 K, $H_2/CO = 1.0$, 5.0 MPa and GHSV = 3600 h^{-1} the best catalyst ($K_1Co_{0.75}MoP$) had a CO conversion of 14.4%, a CH_4 selectivity of 13% and C_2+ oxygenate selectivity of 43%.[135] The K promotion of Mo_2N for synthesis gas conversion to oxygenates has also been reported recently.[136] Catalysts with various K loadings (0.45–6.2 wt%) were operated at 275–325 °C, 7 MPa and 60 000 h^{-1}. The highest total oxygenate selectivity (44% at 300 °C) was observed on a 1.3K-Mo_2N catalyst, but the hydrocarbon selectivity on these catalysts remained high.

1.6 Ammonia and Hydrogen

The ammonia synthesis, $N_2 + 3H_2 \rightarrow 2NH_3$, is an important industrial process used in the manufacture of fertilisers that occurs at 450–500 °C and 30 MPa on Fe catalysts,[3] while the reverse reaction is of current interest because of the potential for NH_3 to be used as a vector for H_2 storage, transportation and supply. Both reactions occur on interstitial metal nitrides and carbides. Ammonia synthesis rates, measured in a stoichiometric H_2/N_2 mixture at atmospheric pressure and 673 K were higher on β-Mo_2C, MoO_xC_y and γ-Mo_2N than on a Ru catalyst, but less than on a K_2O-Fe catalyst.[5] These promising results led to several studies focused on similar materials.[6] In particular, the bimetallic nitrides Fe_3Mo_3N, Co_3Mo_3N and Ni_2Mo_3N have been shown to be highly active for the ammonia synthesis[137,138] and a Cs promoted Co_3Mo_3N catalyst is reported to be more active for ammonia synthesis (15 $mmol\,h^{-1}\,g^{-1}$) at 673 K under 3.1 MPa than a doubly promoted iron catalyst.[139–141] In another recent study, ammonia synthesis under mild conditions (420–500 K, $N_2/H_2 = 1:3$, WHSV of 60 000 $mL\,g^{-1}\,h^{-1}$ and 10 bar) has been demonstrated using LiH-transition metal nitride (V to Ni) composite catalysts, in which the LiH acts as strong reducing agent, which removes activated N atoms from the transition metal nitride, yielding $LiNH_2$ which further reacts with H_2 to yield NH_3 and regenerate the LiH.[142] A Ba-promoted Ru catalysts, supported on BN, has also been used for the ammonia synthesis, with high activities and catalyst stability reported at 360 and 400 °C and at pressures of 50 to 100 bar.[143]

There is significant interest in the production of hydrogen by means other than hydrocarbon reforming/partial oxidation reactions and the use of the interstitial carbides, nitrides and especially the borides as catalysts for these new processes has been proposed in several studies. H_2 production that is free of CO_x is important in the operation of polymer electrolyte membrane (PEM) fuel cells, where the PGM catalysts are readily poisoned by

trace amounts of CO_x. Ammonia decomposition is one approach to obtain CO_x-free H_2 and several studies have focused on metal nitrides and carbides for this reaction. High ammonia decomposition activity of MoN_x/γ-Al_2O_3 and $NiMoN_y/\gamma$-Al_2O_3 catalysts at temperatures 600–750 °C and a GHSV of 1800–3600 h^{-1} was reported by Liang *et al.*[144] who also identified the presence of both Mo_2N and Ni_3Mo_3N phases in the active catalyst. Several other studies of the bimetallic nitrides have since been completed.[145,146] In one case, the activity of a series of bimetallic nitrides was ranked in decreasing order for ammonia decomposition; $Co_3Mo_3N > Ni_3Mo_3N > Fe_3Mo_3N > Mo_2N$.[147] Zheng *et al.*[148] report the use of a Mo_2C catalyst with relatively high activity for ammonia decomposition, as compared to a Ru catalyst as shown in Figure 1.8.

Among the novel methods of hydrogen storage and supply, the hydride salts such as sodium borohydride ($NaBH_4$, NH_3BH_3, $LiBH_4$, *etc.*) are seen as safe hydrogen reservoirs that can readily produce CO_x-free hydrogen by hydrolysis or methanolysis at ambient temperature.[15] Catalysts for the hydrolysis of $NaBH_4$ have been reviewed recently.[15] The most effective catalysts are based on CoB[15,149–151] and for $NaBH_4$ hydrolysis the Co–B is readily promoted by a second metal.[152,153] Patel *et al.* reported that the activity of these materials for $NaBH_4$ hydrolysis decreased in the order

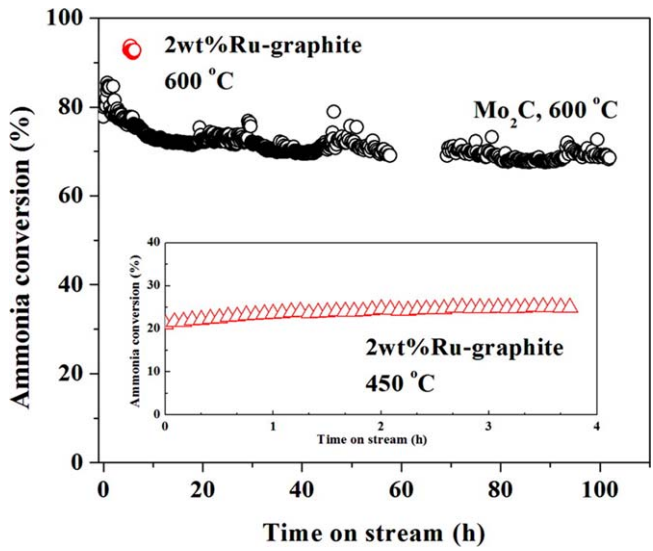

Figure 1.8 Catalytic activity and stability of (circles) Mo carbide and (triangles) graphite-supported 2 wt% Ru catalyst for NH_3 decomposition. Reaction conditions: 50 mg of the sample, NH_3 space velocity 36 000 mL g_{cat}^{-1} min^{-1}, reaction temperature 600 °C (Mo) or 450 °C (Ru).[148]
Reprinted with permission from W. Zheng, T. P. Cotter, P. Kaghazchi, T. Jacob, B. Frank, K. Schlichte, W. Zhang, D. S. Su, F. Schueth and R. Schloegl, *J. Am. Chem. Soc.*, 2013, **135**, 3458–3464 Copyright (2013) American Chemical Society.

Co–Cr–B > Co–Mo–B > Co–W–B > Co–Cu–B > Co–Fe–B > Co–Ni–B > Co–B.[15,154] $NaBH_4$ methanolysis ($NaBH_4 + 4CH_3OH \rightarrow 4H_2 + NaB(OCH_3)_4$) also provides high yields of H_2 and is catalysed by Ru/Al_2O_3, Co/TiO_2, FeB, CuB and MoP. Recently, a significantly higher rate of H_2 evolution per mass of catalyst during $NaBH_4$ methanolysis was reported for a Ni_2P/SiO_2 catalyst, compared to Co and Ru supported on Al_2O_3.[155] Recent efforts to demonstrate H_2 storage and production on a practical scale include the use of a CuB honeycomb catalytic reactor for $NaBH_4$ hydrolysis that produced 7.55 L min^{-1} $g_{Co}{}^{-1}$ at 70 °C.[156] At 134 °C and 5 bar outlet pressure H_2 production of up to 32 L min^{-1} $g_{Co}{}^{-1}$ was obtained.[156]

1.7 Electrocatalysis

The metal carbides have also been the focus of recent developments in electrocatalysis applied to various processes. Water splitting ($H_2O \rightarrow H_2 + \frac{1}{2}O_2$, $\Delta G = 237.1$ kJ mol^{-1}, corresponding to a thermodynamic voltage requirement of 1.23 V)[157] is seen as a promising approach to clean hydrogen. Electrochemical water-splitting includes a cathodic hydrogen evolution reaction (HER; $2H^+ + 2e^- \rightarrow H_2$) and an anodic oxygen evolution reaction (OER; $H_2O \rightarrow \frac{1}{2}O_2 + 2H^+ + 2e^-$). Both the OER and HER reactions require substantial overpotentials and Pt-based metals have the best activity for the HER, and Ru/Ir-based materials are the benchmark catalysts for the OER. Supply and cost issues have meant that there is a major effort aimed at the development of cost-effective and efficient alternative catalytic materials for water splitting. For example, Yu *et al.*[158] describe a new porous carbon-supported Ni/Mo_2C (Ni/Mo_2C-PC) composite catalyst derived from the thermal treatment of nickel molybdate nanorods coated with polydopamine, which catalyses the HER and OER. The catalyst affords small overpotentials of 179 mV for the HER and 368 mV for the OER at a current density of 10 mA cm^{-2}. The home-made alkaline electrolyser, assembled with Ni/Mo_2C-PC as a bifunctional catalyst, can enable a water-splitting current density of 10 mA cm^{-2} to be achieved at a low cell voltage of 1.66 V. In another study, the use of a WC catalyst co-doped with Co and N, for both oxygen reduction reaction (ORR) and hydrogen evolution reaction (HER), is reported.[159] In other cases the metal carbide such as TiC has been used as a support for single atom metal catalysts, such as Pt on TiC used for the ORR. In a recent report, Co_2B was shown to be an excellent catalyst for the OER and is simultaneously active for catalysing the HER.[160,161] The catalyst achieves a current density of 10 mA cm^{-2} at 1.61 V on an inert support and at 1.59 V when impregnated with nitrogen-doped graphene.[160,161]

Metal carbides have also been used on other electrochemical processes, including Mo_2C which is capable of catalysing CO_2 conversion to CH_4 at low potentials[162] and a Fe–N–C catalyst, that includes graphitic carbon, graphene, iron carbides, FeN and Fe_2N and that is suitable for SO_2 electrooxidation.[163]

1.8 Conclusions

The metal carbides, nitrides, phosphides and borides have shown promise as new catalysts for a range of reactions normally catalysed by metals. The behaviour of these new materials is attributable to changes in the electronic properties of the metal surface induced by the ligands and by the metal–ligand surface geometry. The materials are active in catalytic hydrogenations, hydrotreating and synthesis gas production and conversion. In several cases, they provide unique reaction pathways and are more active or selective than conventional metal catalysts. Nevertheless, commercial application remains a challenge. The stability of the materials under the relatively severe reaction conditions encountered in hydrotreating and synthesis gas conversion, for example, is low, resulting in changes to the surface composition of the catalysts. Promising results have been reported in electrocatalytic applications such as water splitting and hydrogen production. The rich chemistry of these materials provides an opportunity for further discovery and development, with the potential to apply these materials to a range of unexplored catalytic reactions.

References

1. I. Chorkendorff and J. W. Niemantsverdriet, *Concepts of Modern Catalysis and Kinetics*, Wiley-VCH, Weinheim, 2007.
2. M. J. Ledoux, C. Pham-Huu and R. R. Chianelli, *Curr. Opin. Solid State Mater. Sci.*, 1996, **1**, 96–100.
3. C. H. Bartholomew and R. J. Farrauto, *Fundamentals of Industrial Catalytic Processes*, Wiley, Hoboken, NJ, 2006.
4. R. B. Levy and M. Boudart, *Science*, 1973, **181**, 547–549.
5. S. T. Oyama, *Catal. Today*, 1992, **15**, 179–200.
6. J. S. J. Hargreaves, *Coord. Chem. Rev.*, 2013, **257**, 2015–2031.
7. R. Prins and M. E. Bussell, *Catal. Lett.*, 2012, **142**, 1413–1436.
8. H. H. Hwu and J. G. Chen, *Chem. Rev.*, 2005, **105**, 185–212.
9. S. T. Oyama, T. Gott, H. Zhao and Y. Lee, *Catal. Today*, 2009, **143**, 94–107.
10. S. Zaman and K. J. Smith, *Catal. Rev.*, 2012, **54**, 41–132.
11. P. Liu and J. A. Rodriguez, *Catal. Lett.*, 2003, **91**, 247–252.
12. J. G. Chen, B. Fruhberger, J. Eng Jr. and B. E. Bent, *J. Mol. Catal. A: Chem.*, 1998, **131**, 285–299.
13. E. Furimsky, *Appl. Catal., A*, 2003, **240**, 1–28.
14. M. Nagai, *Appl. Catal., A*, 2007, **322**, 178–190.
15. N. Patel and A. Miotello, *Int. J. Hydrogen Energy*, 2015, **40**, 1429–1464.
16. I. I. Abu and K. J. Smith, *J. Catal.*, 2006, **241**, 356–366.
17. M. M. Sullivan, J. T. Held and A. Bhan, *J. Catal.*, 2015, **326**, 82–91.
18. M. M. Sullivan and A. Bhan, *J. Catal.*, 2016, **344**, 53–58.
19. G. Horanyi, G. Vertes and G. Fezler, *Z. Phys. Chem.*, 1973, **83**, 322–324.
20. G. Horanyi and G. Vertes, *J. Chem. Soc., Perkin Trans. 2*, 1975, 827–829.

21. G. Horanyi and E. M. Rizmayer, *React. Kinet. Catal. Lett.*, 1980, **13**, 21–26.
22. I. Kojima, E. Miyazaki, Y. Inoue and I. Yasumori, *J. Catal.*, 1979, **59**, 472–474.
23. Y. Li, Y. Fan, J. He, B. Xu, H. Yang, J. Miao and Y. Chen, *Chem. Eng. J.*, 2004, **99**, 213–218.
24. H. Imamura, T. Nuruyu, T. Kawasaki, T. Teranishi and Y. Sakata, *Catal. Lett.*, 2004, **96**, 185–187.
25. N. Perret, A. Alexander, S. M. Hunter, P. Chung, J. S. J. Hargreaves, R. F. Howe and M. A. Keane, *Appl. Catal., A*, 2014, **488**, 128–137.
26. C. Barnett, *Ind. Eng. Chem. Prod. Res. Develop.*, 1969, **8**, 145–149.
27. Y. Nitta, T. Imanaka and S. Teranishi, *Bull. Chem. Soc. Jpn.*, 1980, **53**, 3154–3158.
28. J. Choi and N. M. Yoon, *Synthesis*, 1996, 597–599.
29. M. Pang, C. Liu, W. Xia, M. Muhler and C. Liang, *Green Chem.*, 2012, **14**, 1272–1276.
30. S. J. Ardakani, X. Liu and K. J. Smith, *Appl. Catal., A*, 2007, **324**, 9–19.
31. L. Zhang, J. Feng, Q. Chu, W. Li, K. Xu and T. S. Wiltowski, *Catal. Commun.*, 2015, **66**, 50–54.
32. Z. Liu, S. Xie, B. Liu and J. Deng, *New J. Chem.*, 1999, **23**, 1057.
33. M. Frauwallner, F. Lopez-Linares, J. Lara-Romero, C. E. Scott, V. Ali, E. Hernandez and P. Pereira-Almao, *Appl. Catal., A*, 2011, **394**, 62–70.
34. S. Qi, J. Yue, Y. Y. Li, J. Huang, C. Yi and B. L. Yang, *Catal. Lett.*, 2014, **144**, 1443–1449.
35. J. Choi and N. M. Yoon, *Tetrahedron Lett.*, 1996, **37**, 1057–1060.
36. W. Wang, M. Qiao, J. Yang, S. Xie and J. Deng, *Appl. Catal., A*, 1997, **163**, 101–109.
37. Y. Nakao and S. Fujishige, *J. Catal.*, 1981, **68**, 406–410.
38. Z. Wu, C. Li, P. Ying, Z. Wei and Q. Xin, *Chem. Commun.*, 2001, 1048.
39. J. Quiroz, E. F. Mai and D. S. Teixeira, *Top. Catal.*, 2016, **59**, 148–158.
40. W. Luo, U. Deka, A. M. Beale, R. H. E. van Eck, P. C. A. Bruijnincx and B. M. Weckhuysen, *J. Catal.*, 2013, **301**, 175–186.
41. K. Shimizu, S. Kanno and K. Kon, *Green Chem.*, 2014, **16**, 3899–3903.
42. B. Liaw, M. Lee and Y. Chen, *J. Chin. Inst. Chem. Eng.*, 2003, **34**, 667–674.
43. S. Chiang, C. Yang, Y. Chen and B. Liaw, *Appl. Catal., A*, 2007, **326**, 180–188.
44. B. Liaw, C. Chen and Y. Chen, *Chem. Eng. J.*, 2010, **157**, 140–145.
45. H. Li and J. Deng, *J. Chem. Technol. Biotechnol.*, 2001, **76**, 985–990.
46. H. Li, H. Li and J. Deng, *Catal. Today*, 2002, **74**, 53–63.
47. G. Luo, S. Yan, M. Qiao and K. Fan, *Appl. Catal., A*, 2007, **332**, 79–88.
48. F. Cardenas-Lizana, S. Gomez-Quero, N. Perret, L. Kiwi-Minsker and M. A. Keane, *Catal. Sci. Technol.*, 2011, **1**, 118–125.
49. F. Taghavi, C. Falamaki, A. Shabanov, L. Bayrami and A. Roumianfar, *Appl. Catal., A*, 2011, **407**, 173–180.
50. M. K. Neylon, S. Choi, H. Kwon, K. E. Curry and L. T. Thompson, *Appl. Catal., A*, 1999, **183**, 253–263.

51. Y. Liu and Y. Chen, *Ind. Eng. Chem. Res.*, 2006, **45**, 2973–2980.
52. Y. Chen and N. Sasirekha, *Ind. Eng. Chem. Res.*, 2009, **48**, 6248–6255.
53. B. Zhao and Y. Chen, *Mater. Chem. Phys.*, 2011, **125**, 763–768.
54. Y. Liu, J. Ding, J. Sun, J. Zhang, J. Bi, K. Liu, F. Kong, H. Xiao, Y. Sun and J. Chen, *Chem. Commun.*, 2016, **52**, 5030–5032.
55. Y. Liu, J. Ding, J. Bi, Y. Sun, J. Zhang, K. Liu, F. Kong, H. Xiao and J. Chen, *Appl. Catal., A*, 2017, **529**, 143–155.
56. T. Kabe, A. Ishihara and W. Qian, *Hydrodesulfurization and Hydrodenitrogenation*, Wiley-VCH, Weinheim, 2000.
57. S. T. Oyama, *J. Catal.*, 2003, **216**, 343–352.
58. S. E. Skrabalak and K. S. Suslick, *Chem. Mater.*, 2006, **18**, 3103–3107.
59. P. Bui, J. A. Cecilia, S. T. Oyama, A. Takagaki, A. Infantes-Molina, H. Zhao, D. Li, E. Rodríguez-Castellón and A. Jiménez López, *J. Catal.*, 2012, **294**, 184–198.
60. K. Xiong, W. Yu, D. G. Vlachos and J. G. Chen, *ChemCatChem*, 2015, **7**, 1402–1421.
61. D. J. Sajkowski and S. T. Oyama, *Appl. Catal., A*, 1996, **134**, 339–349.
62. Y. Villasana, Y. Escalante, J. E. Rodriguez Nunez, F. J. Mendez, S. Ramirez, M. Luis-Luis, E. Canizales, J. Ancheyta and J. L. Brito, *Catal. Today*, 2014, **220–222**, 318–326.
63. V. Sundaramurthy, A. K. Dalai and J. Adjaye, *Appl. Catal., A*, 2006, **311**, 155–163.
64. V. Sundaramurthy, A. K. Dalai and J. Adjaye, *Catal. Today*, 2007, **125**, 239–247.
65. V. Sundaramurthy, A. K. Dalai and J. Adjaye, *Appl. Catal., A*, 2008, **335**, 204–210.
66. P. Da Costa, C. Potvin, J. Manoli, B. Genin and G. Djega-Mariadassou, *Fuel*, 2004, **83**, 1717–1726.
67. S. T. Oyama, X. Wang, F. G. Requejo, T. Sato and Y. Yoshimura, *J. Catal.*, 2002, **209**, 1–5.
68. I. I. Abu and K. J. Smith, *Appl. Catal., A*, 2007, **328**, 58–67.
69. K. K. Soni, P. E. Boahene and A. K. Dalai, *Prepr. - Am. Chem. Soc., Div. Pet. Chem.*, 2012, **57**, 21–23.
70. K. K. Soni, P. E. Boahene and A. K. Dalai, *Prepr. Symp. - Am. Chem. Soc., Div. Fuel Chem.*, 2011, **56**, 315–316.
71. P. Da Costa, C. Potvin, J.- Manoli, M. Breysse and G. Djega-Mariadassou, *Catal. Lett.*, 2003, **86**, 133–138.
72. P. Da Costa, C. Potvin, J. Manoli, J. Lemberton, G. Perot and G. Djega-Mariadassou, *J. Mol. Catal. A: Chem.*, 2002, **184**, 323–333.
73. S. Ramanathan and S. T. Oyama, *J. Phys. Chem.*, 1995, **99**, 16365–16372.
74. I. K. Milad, K. J. Smith, P. C. Wong and K. A. R. Mitchell, *Catal. Lett.*, 1998, **52**, 113–119.
75. E. Furimsky, *Appl. Catal., A*, 2000, **199**, 147–190.
76. A. L. Jongerius, R. W. Gosselink, J. Dijkstra, J. H. Bitter, P. C. A. Bruijnincx and B. M. Weckhuysen, *ChemCatChem*, 2013, **5**, 2964–2972.

77. W. Lee, Z. Wang, R. J. Wu and A. Bhan, *J. Catal.*, 2014, **319**, 44–53.
78. Q. Lu, C. Chen, W. Luc, J. G. Chen, A. Bhan and F. Jiao, *ACS Catal.*, 2016, **6**, 3506–3514.
79. C. Sepúlveda, K. Leiva, R. García, L. R. Radovic, I. T. Ghampson, W. J. DeSisto, J. L. G. Fierro and N. Escalona, *Catal. Today*, 2011, **172**, 232–239.
80. I. Tyrone Ghampson, C. Sepulveda, R. Garcia, J. L. Garcia Fierro, N. Escalona and W. J. DeSisto, *Appl. Catal., A*, 2012, **435–436**, 51–60.
81. I. T. Ghampson, C. Sepulveda, R. Garcia, B. G. Frederick, M. C. Wheeler, N. Escalona and W. J. DeSisto, *Appl. Catal., A*, 2012, **413–414**, 78–84.
82. H. Y. Zhao, D. Li, P. Bui and S. T. Oyama, *Appl. Catal., A*, 2011, **391**, 305–310.
83. V. M. L. Whiffen and K. J. Smith, *Energy Fuels*, 2010, **24**, 4728–4737.
84. S. Boullosa-Eiras, R. Lødeng, H. Bergem, M. Stöcker, L. Hannevold and E. A. Blekkan, *Catal. Today*, 2014, **223**, 44–53.
85. J. Chang, T. Danuthai, S. Dewiyanti, C. Wang and A. Borgna, *ChemCatChem*, 2013, **5**, 3041–3049.
86. C. A. Teles, R. Rabelo-Neto, J. R. de Lima, L. V. Mattos, D. E. Resasco and F. B. Noronha, *Catal. Lett.*, 2016, **146**, 1848–1857.
87. C. Chiu, A. Genest, A. Borgna and N. Rösch, *ACS Catal.*, 2014, **4**, 4178–4188.
88. C. Guo, V. R. Tirumala, E. Reyhanitash, Z. Yuan, S. Rohani, C. Xu and S. He, *AIChE J.*, 2016, **62**, 3664–3672.
89. C. Kordulis, K. Bourikas, M. Gousi, E. Kordouli and A. Lycourghiotis, *Appl. Catal., B*, 2016, **181**, 156–196.
90. J. Han, J. Duan, P. Chen, H. Lou and X. Zheng, *Adv. Synth. Catal.*, 2011, **353**, 2577–2583.
91. J. Han, J. Duan, P. Chen, H. Lou, X. Zheng and H. Hong, *ChemSusChem*, 2012, **5**, 727–733.
92. J. Monnier, H. Sulimma, A. Dalai and G. Caravaggio, *Appl. Catal., A*, 2010, **382**, 176–180.
93. Q. Guan, F. Wan, F. Han, Z. Liu and W. Li, *Catal. Today*, 2016, **259**, 467–473.
94. F. Han, Q. Guan and W. Li, *RSC Adv.*, 2015, **5**, 107533–107539.
95. H. Shi, J. Chen, Y. Yang and S. Tian, *Fuel Process. Technol.*, 2014, **118**, 161–170.
96. G. Shi, L. Su and K. Jin, *Catal. Commun.*, 2015, **59**, 180–183.
97. C. Li, M. Zheng, A. Wang and T. Zhang, *Energy Environ. Sci.*, 2012, **5**, 6383–6390.
98. R. Ma, W. Hao, X. Ma, Y. Tian and Y. Li, *Angew. Chem., Int. Ed. Engl.*, 2014, **53**, 7310–7315.
99. X. Ma, Y. Tian, W. Hao, R. Ma and Y. Li, *Appl. Catal., A*, 2014, **481**, 64–70.
100. N. Ji, T. Zhang, M. Zheng, A. Wang, H. Wang, X. Wang, Y. Shu, A. L. Stottlemyer and J. G. Chen, *Catal. Today*, 2009, **147**, 77–85.
101. D. C. LaMont and W. J. Thomson, *Chem. Eng. Sci.*, 2005, **60**, 3553–3559.

102. A. J. Brungs, A. P. E. York, J. B. Claridge, C. Márquez-Alvarez and M. L. H. Green, *Catal. Lett.*, 2000, **70**, 117–122.
103. C. Song and W. Pan, *Catal. Today*, 2004, **98**, 463–484.
104. J. Garcia-Vargas, J. L. Valverde, A. de Lucas-Consuegra, B. Gomez-Monedero, F. Dorado and P. Sanchez, *Int. J. Hydrogen Energy*, 2013, **38**, 4524–4532.
105. J. Garcia-Vargas, J. L. Valverde, J. Diez, F. Dorado and P. Sanchez, *Int. J. Hydrogen Energy*, 2015, **40**, 8677–8687.
106. W. Li, Z. Zhao, P. Ren and G. Wang, *RSC Adv.*, 2015, **5**, 100865–100872.
107. A. Brush, E. J. Evans Jr., G. M. Mullen, K. Jarvis and C. B. Mullins, *Fuel Process. Technol.*, 2016, **153**, 111–120.
108. G. Wang, J. A. Schaidle, M. B. Katz, Y. Li, X. Pan and L. T. Thompson, *J. Catal.*, 2013, **304**, 92–99.
109. N. M. Schweitzer, J. A. Schaidle, O. K. Ezekoye, X. Pan, S. Linic and L. T. Thompson, *J. Am. Chem. Soc.*, 2011, **133**, 2378–2381.
110. K. D. Sabnis, Y. Cui, M. C. Akatay, M. Shekhar, W. Lee, J. T. Miller, W. N. Delgass and F. H. Ribeiro, *J. Catal.*, 2015, **331**, 162–171.
111. E. de Smit and B. M. Weckhuysen, *Chem. Soc. Rev.*, 2008, **37**, 2758–2781.
112. A. Y. Khodakov, W. Chu and P. Fongarland, *Chem. Rev.*, 2007, **107**, 1692–1744.
113. R. B. Anderson, H. Kölbel and M. Rálek, *The Fischer-Tropsch Synthesis*. Academic Press, Orlando, 1984.
114. A. Trovarelli, P. Matteazzi, G. Dolcetti, A. Lutman and F. Miani, *Appl. Catal., A*, 1993, **95**, L13.
115. J. Blanchard, N. Abatzoglou, R. Eslahpazir-Esfandabadi and F. Gitzhofer, *Ind. Eng. Chem. Res.*, 2010, **49**, 6948–6955.
116. E. de Smit, F. Cinquini, A. M. Beale, O. V. Safonova, W. van Beek, P. Sautet and B. M. Weckhuysen, *J. Am. Chem. Soc.*, 2010, **132**, 14928–14941.
117. X. Huo, Z. Wang, J. Huang, R. Zhang and Y. Fang, *Catal. Commun.*, 2016, **79**, 39–44.
118. X. Huo, Z. Wang, J. Huang, R. Zhang and Y. Fang, *RSC Adv.*, 2016, **6**, 24353–24360.
119. K. Y. Park, W. K. Seo and J. S. Lee, *Catal. Lett.*, 1991, **11**, 349–356.
120. D. N. Vo and A. A. Adesina, *Catal. Sci. Technol.*, 2012, **2**, 2066–2076.
121. D. N. Vo, C. G. Cooper, T. Nguyen, A. A. Adesina and D. B. Bukur, *Fuel*, 2012, **93**, 105–116.
122. D. N. Vo, V. Arcotumapathy, B. Abdullah and A. A. Adesina, *J. Chem. Technol. Biotechnol.*, 2013, **88**, 1358–1363.
123. D. N. Vo and A. A. Adesina, *ACS Symp. Ser.*, 2011, **1084**, 155–184.
124. D. N. Vo, T. Nguyen, E. M. Kennedy, B. Z. Dlugogorski and A. A. Adesina, *Catal. Today*, 2011, **175**, 450–459.
125. N. Wang, K. Fang, D. Jiang, D. Li and Y. Sun, *Catal. Today*, 2010, **158**, 241–245.
126. M. Xiang, D. Li, W. Li, B. Zhong and Y. Sun, *Fuel*, 2006, **85**, 2662–2665.

127. M. Xiang, D. Li, H. Qi, W. Li, B. Zhong and Y. Sun, *Fuel*, 2007, **86**, 1298–1303.
128. M. Xiang, D. Li, H. Xiao, J. Zhang, H. Qi, W. Li, B. Zhong and Y. Sun, *Fuel*, 2008, **87**, 599–603.
129. L. Zhao, K. Fang, D. Jiang, D. Li and Y. Sun, *Catal. Today*, 2010, **158**, 490–495.
130. Q. Wu, J. M. Christensen, G. L. Chiarello, L. D. L. Duchstein, J. B. Wagner, B. Temel, J. Grunwaldt and A. D. Jensen, *Catal. Today*, 2013, **215**, 162–168.
131. Y. Chen, B. Liaw and B. Chen, *Appl. Catal., A*, 2002, **236**, 121–128.
132. B. J. Liaw and Y. Z. Chen, *Appl. Catal., A*, 2001, **206**, 245–256.
133. S. F. Zaman and K. J. Smith, *Appl. Catal., A*, 2010, **378**, 59–68.
134. S. F. Zaman and K. J. Smith, *Catal. Commun.*, 2009, **10**, 468–471.
135. R. Xu, Y. Li, Z. Cao, J. Zheng, N. Zhang, B. Chen and W. Wang, *Catal. Commun.*, 2014, **51**, 63–67.
136. S. F. Zaman, N. Pasupulety, A. A. Al-Zahrani, M. A. Daous, S. S. Al-Shahrani, H. Driss, L. A. Petrov and K. J. Smith, *Appl. Catal., A*, 2017, **532**, 133–145.
137. C. J. H. Jacobsen, *Chem. Commun.*, 2000, 1057–1058.
138. A. Boisen, S. Dahl and C. J. H. Jacobsen, *J. Catal.*, 2002, **208**, 180–186.
139. R. Kojima and K. Aika, *Chem. Lett.*, 2000, 514–515.
140. R. Kojima and K.- Aika, *Appl. Catal., A*, 2001, **215**, 149–160.
141. R. Kojima and K.- Aika, *Appl. Catal., A*, 2001, **218**, 121–128.
142. P. Wang, F. Chang, W. Gao, J. Guo, G. Wu, T. He and P. Chen, *Nat. Chem.*, 2017, **9**, 64–70.
143. C. J. H. Jacobsen, *J. Catal.*, 2001, **200**, 1–3.
144. C. Liang, W. Li, Z. Wei, Q. Xin and C. Li, *Ind. Eng. Chem. Res.*, 2000, **39**, 3694–3697.
145. D. V. Leybo, A. N. Baiguzhina, D. S. Muratov, D. I. Arkhipov, E. A. Kolesnikov, V. V. Levina, N. I. Kosova and D. V. Kuznetsov, *Int. J. Hydrogen Energy*, 2016, **41**, 3854–3860.
146. S. Podila, S. F. Zaman, H. Driss, Y. A. Alhamed, A. Al-Zahrani and L. A. Petrov, *Catal. Sci. Technol.*, 2016, **6**, 1496–1506.
147. A. Srifa, K. Okura, T. Okanishi, H. Muroyama, T. Matsui and K. Eguchi, *Catal. Sci. Technol.*, 2016, **6**, 7495–7504.
148. W. Zheng, T. P. Cotter, P. Kaghazchi, T. Jacob, B. Frank, K. Schlichte, W. Zhang, D. S. Su, F. Schueth and R. Schloegl, *J. Am. Chem. Soc.*, 2013, **135**, 3458–3464.
149. G. M. Arzac, D. Hufschmidt, J. D. Haro, A. Fernandez, B. Sarmiento, M. A. Jimenez and M. M. Jimenez, *Int. J. Hydrogen Energy*, 2012, **37**, 14373–14381.
150. J. Delmas, L. Laversenne, I. Rougeaux, P. Capron, A. Garron, S. Bennici, D. Swierczynski and A. Auroux, *Int. J. Hydrogen Energy*, 2011, **36**, 2145–2153.
151. X. Shen, M. Dai, M. Gao, B. Zhao and W. Ding, *Cuihua Xuebao*, 2013, **34**, 979–985.

152. Z. Wu, X. Mao, Q. Zi, R. Zhang, T. Dou and A. C. K. Yip, *J. Power Sources*, 2014, **268**, 596–603.
153. N. Patel and A. Miotello, *Int. J. Hydrogen Energy*, 2015, **40**, 1429–1464.
154. N. Patel, R. Fernandes and A. Miotello, *J. Catal.*, 2010, **271**, 315–324.
155. K. Yan, Y. Li, X. Zhang, X. Yang, N. Zhang, J. Zheng, B. Chen and K. J. Smith, *Int. J. Hydrogen Energy*, 2015, **40**, 16137–16146.
156. A. Marchionni, M. Bevilacqua, J. Filippi, M. G. Folliero, M. Innocenti, A. Lavacchi, H. A. Miller, M. V. Pagliaro and F. Vizza, *J. Power Sources*, 2015, **299**, 391–397.
157. J. D. Benck, T. R. Hellstern, J. Kibsgaard, P. Chakthranont and T. F. Jaramillo, *ACS Catal.*, 2014, **4**, 3957–3971.
158. Z. Yu, Y. Duan, M. Gao, C. Lang, Y. Zheng and S. Yu, *Chem. Sci.*, 2016, DOI: 10.1039/C6SC03356C.
159. S. Bukola, B. Merzougui, A. Akinpelu and M. Zeama, *Electrochim. Acta*, 2016, **190**, 1113–1123.
160. J. Masa, P. Weide, D. Peeters, I. Sinev, W. Xia, Z. Sun, C. Somsen, M. Muhler and W. Schuhmann, *Adv. Energy Mater.*, 2016, **6**, DOI: 10.1002/aenm.201502313.
161. J. Masa, P. Weide, D. Peeters, I. Sinev, W. Xia, Z. Sun, C. Somsen, M. Muhler and W. Schuhmann, *Adv. Energy Mater.*, 2016, **6**, 1670072.
162. S. K. Kim, Y. Zhang, H. Bergstrom, R. Michalsky and A. Peterson, *ACS Catal.*, 2016, **6**, 2003–2013.
163. Q. Zhao, M. Hou, S. Jiang, S. Wang, J. Ai, L. Zheng and Z. Shao, *RSC Adv.*, 2016, DOI: 10.1039/C6RA16872H. Ahead of Print.
164. D. L. Nguyen, P. Leroi, M. J. Ledoux and C. Pham-Huu, *Catal. Today*, 2009, **141**, 393–396.
165. J. R. H. Ross, *Catal. Today*, 2005, **100**, 151–158.
166. H. Shao, E. L. Kugler, W. Ma and D. B. Dadyburjor, *Ind. Eng. Chem. Res.*, 2005, **44**, 4914–4921.
167. S. Zhang, C. Shi, B. Chen, Y. Zhang, Y. Zhu, J. Qiu and C. Au, *Catal. Today*, 2015, **258**, 676–683.
168. X. Du, L. J. France, V. L. Kuznetsov, T. Xiao, P. P. Edwards, H. Al Megren and A. Bagabas, *Appl. Petrochem. Res.*, 2014, **4**, 137–144.
169. Z. Yao, J. Jiang, Y. Zhao, F. Luan, J. Zhu, Y. Shi, H. Gao and H. Wang, *RSC Adv.*, 2016, **6**, 19944–19951.